



Evaluation of Asphalt Overlay Properties on Reflection Cracking Behavior of Composite Pavement Using Finite Element Modeling

Received 11 September 2024; Revised 16 December 2024; Accepted 16 December 2024

Mohamed Gamal¹
Mahmoud Enieb²
Elsayed M Abd Alla³

Keywords

Finite Elements Analysis
Pavement Modeling
Reflection Cracking
Asphalt Overlaying

Abstract: Reflective cracking poses a significant challenge to the performance and durability of Hot-Mix Asphalt (HMA) overlays, particularly when applied over deteriorated Joint Plain Concrete (JPC) pavements. This study explores the effects of reflective cracking on overlay pavements through Finite Element Analysis (FEA) using ABAQUS, integrating the Cohesive Zone Model (CZM) to simulate crack initiation and propagation. Key factors analysed include overlay thickness, modulus of elasticity, JPC joint width, and fracture areas within the pavement structure. The results indicate that increasing overlay thickness from 30 mm to 100 mm reduces tensile strain by up to 68.8%, significantly improving stress dissipation. Variations in the modulus of elasticity (ranging from 1500 MPa to 6000 MPa) were found to reduce tensile strain by approximately 37.5%. Additionally, the number of load repetitions required to cause reflective cracking increases with overlay thickness: 11,220 repetitions for 30 mm, 226,458 repetitions for 60 mm, and 458,835 repetitions for 100 mm. Wider JPC joints (from 6 mm to 20 mm) increased stress concentrations and crack severity. The study also quantified fracture behavior using the Representative Fracture Area (RFA), with RFA increasing by up to 99% under higher load repetitions. These findings provide practical recommendations for pavement design, particularly in selecting optimal overlay thicknesses and material properties to extend the lifespan of rehabilitated pavements and mitigate reflective cracking.

1. Introduction

Overlay is often preferred to restore pavement structure and improve ride quality with asphalt concrete overlay being a standard technique for rehabilitating rigid pavements. This approach, widely known for its effectiveness, faces the challenge of reflective cracking, which occurs when the asphalt surface is subjected to stresses or strains caused by bending and displacement of the concrete at existing joints or cracks. These cracks, often caused by temperature fluctuations, humidity, and traffic loads, lead to early failure and significantly reduce the performance and maintainability of the coating

¹ Civil Engineering Dept., Al-Safwa High Institute of Engineering, Cairo, Egypt. mohamedgamal@engineer.com

² Professor, Civil Engineering Dept., Assiut University, Assiut, Egypt. m.enieb@aun.edu.eg

³ Professor, Civil Engineering Dept., Assiut University, Assiut, Egypt. elsayed.mohamed1@aun.edu.eg

[1]. The main problem is increased tensile strains at the bottom of the AC layer near cracks and joints. Extensive research has been conducted to understand how these critical responses vary with changes in pavement properties (e.g., structure and material properties) using methods such as accelerated pavement testing, laboratory studies, and numerical analysis. Considering AC overlay modulus, modulus of existing pavements, dimension of joints, and the thickness of the overlay layer, these factors are all crucial to influencing the effectiveness of a deck at different levels [1-6]. The overall performance of pavement structures can be significantly impacted by severe reflective cracking in asphalt overlays. To properly apply targeted treatments that reduce the dangers related to asphalt overlays, it is imperative to determine the size of reflecting cracks in advance [7]. To estimate reflective cracking in asphalt overlays, several predictive models using empirical, mechanistic, or combination empirical-mechanistic approaches have been developed. To determine the severity of cracks, these models make use of field data and fracture mechanics principles. Conventional fracture mechanics usually assume homogeneous crack propagation in stress or strain plane scenarios, which results in simple crack depth predictions for asphalt overlays cracks may propagate non-uniformly across the cross-sectional area of the asphalt overlay under real-world situations like wheel stresses. This implies that interpreting crack propagation incorrectly could arise from depending only on conventional assumptions [7]. This research investigates the possibility of simulating the real conditions in which reflective cracking occurs. Predictive models for reflective cracks, whether based on mathematical derivations or laboratory results, sometimes lack accuracy because laboratory conditions do not necessarily represent the actual conditions of road operation. This research provides valuable insights for road engineers by helping them design more durable Hot Mix Asphalt (HMA) overlays through the selection of optimal thickness and material properties, directly influencing pavement rehabilitation decisions. Road maintenance projects can become more cost-efficient, reducing the frequency and costs of repairs and ultimately leading to better resource allocation. Additionally, the study offers insights into the long-term performance of rehabilitated pavements under varying conditions, aiding in the forecasting of maintenance schedules and extending pavement lifespan, making the findings highly applicable in real-world scenarios. The higher the temperature applied to the flexible pavement layer, the lower the elastic modulus value will be. In contrast, the elastic modulus of the pavement layer decreases as the temperature increases, as shown in Fig. 1[8].

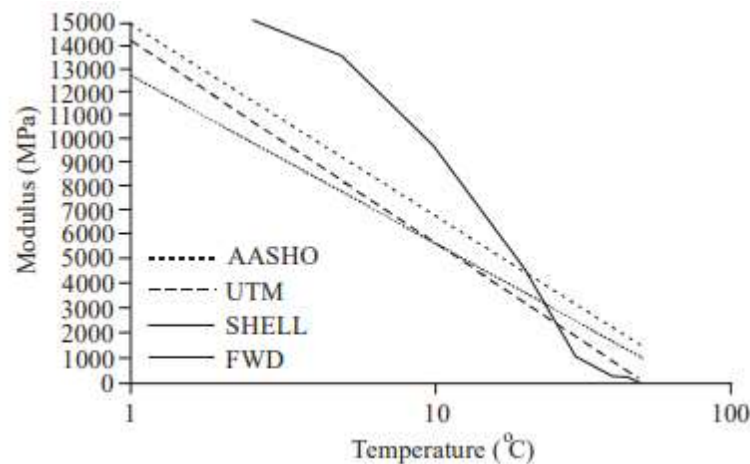


Fig. 1: Asphalt moduli versus temperature [8].

Several techniques, such as Cohesive Zone Modeling (CZM), the Extended Finite Element Method (XFEM), and Stress Intensity Factor (SIF) cracking models, can be employed to model reflective cracking due to advancements in road engineering and simulation methods, including the use of Finite Element Analysis (FEA), Artificial Neural Networks (ANN), and empirical mechanisms. The cohesive zone method was used in this paper's simulation because it has the benefit of simulating non-linear fractures. It has also been extensively employed in fracture simulations. To assess how well some solutions to the problem of reflective cracks work [3, 9-11]. The cohesive zone model (CZM) is increasingly used in finite element (FE) simulations to understand the fracture behavior of asphalt concrete materials. Key fracture properties required for these models include local fracture energy (G_f) and material strength (σ_c). Among the various methods proposed for measuring the fracture energy of asphalt mixtures, the Disk-Shaped Compact Tension DCT Test, standardized as ASTM D7313-13, is one of the earliest and most widely adopted procedures. The CZM method had been successfully used for modeling the Disk-shaped Compact Tension (DCT) Test, as demonstrated by Baek as shown in Fig. 2 [7, 12].

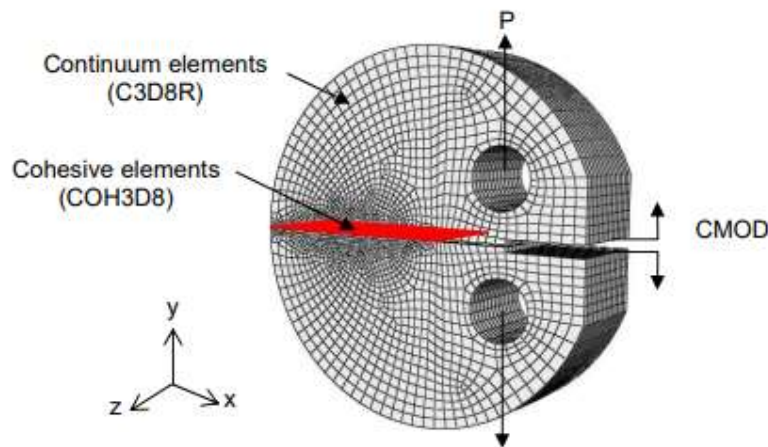


Fig. 2:Finite elements model for DCT test [7].

2. Cohesive Zone Model CZM

Cohesive Zone Model CZM was utilized in this study to evaluate the uneven development of reflective fractures in asphalt overlays. The effectiveness of this model in taking the nonlinear behaviour of the material during the cracking process has been acknowledged. As mentioned in earlier research, a bilinear traction-separation law was also used to characterize the fracture behaviour of the asphalt material. Certain parameters, such as the tensile strength (σ_t) and fracture energy (G_f) of the asphalt overlay, can be determined for this constitutive model. The properties of the cohesive elements were further defined based on their stiffness in the normal (K_n), first shear (K_s), and second shear (K_t) directions, providing a comprehensive framework for understanding the mechanics of crack propagation in layered pavement structures. Since the compliance issue of the cohesive zone was minimal, the cohesive element stiffness used in this study was equivalent to the asphalt modulus [7, 13-16]. In this study, the tensile stress for the asphalt was assumed to be around 900 Newtons, and the fracture energy was approximately 590 N/m, based on the works of Ding [17].

3. Representative Fracture Area (RFA)

This research also introduced the concept of non-uniform crack propagation for assessing potential reflective cracks. The propagation of these cracks was quantified using the Representative Fracture Area (RFA), which is the ratio of the damaged area to the total cross-sectional area of the asphalt overlay. This approach effectively determined the actual formation of cracks in the asphalt overlay under the influence of wheel loads [7, 9, 11].

The fracture behaviour of reflective cracking was examined using a scalar stiffness degradation parameter, which quantifies damage within a cohesive element. This parameter expresses the loss of stiffness due to cracking: a value of 0 indicates that the material retains its full stiffness (no damage), while a value of 1 represents zero stiffness (complete failure). The degradation contours are illustrated in the in-plane area with zero thickness of the cohesive elements (1750 mm length and 60 mm height) that lie perpendicular to traffic direction and above a transverse joint. Furthermore, the Representative Fracture Area (RFA) was introduced to evaluate the non-uniform crack propagation in asphalt overlays under traffic loads. This approach, challenges traditional views on crack propagation. Influenced by the scalar stiffness degradation, the area of the cohesive element, and the total cross-sectional area of the overlay as outlined in Equation (1), the RFA % ranges from 0 (no crack) to 100% (fully developed crack). Calculated through mechanistic analysis in ABAQUS, it tracks the progression of material stiffness degradation from undamaged to fully damaged, as shown in Fig. 3.

$$RFA_{overlay} = \left(\frac{\sum_{j=1}^Z \sum_{i=1}^X |(A_{cohesive})_{ij} D_{ij}|}{A_{overlay}} \right) \times 100 \quad (1)$$

The $RFA_{overlay}$ represents the fractured area of the complete HMA overlay. $A_{cohesive}$ Is the original in-plane area of a cohesive element placed in row i and column j. D_{ij} is the stiffness degradation parameter for a certain cohesive element. X and Z represent the total number of cohesive elements in the depth and transverse direction. Fig. 4 also shows the distribution of cohesive elements across rows (i) and columns (j) within the overlay, highlighting the original in-plane area $A_{cohesive}$ of each cohesive element.

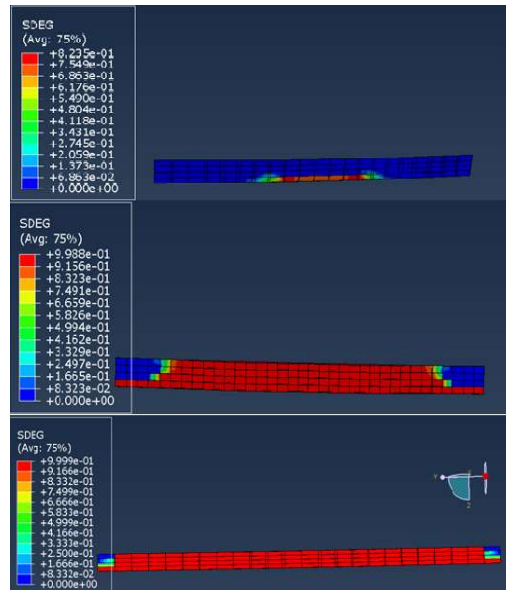


Fig. 3: The stiffness degradation parameter for a certain cohesive element under different load values.

Cohesive Element Layout with Enlarged Text (i vs. j)

	i=1 j=1	i=2 j=1	i=3 j=1	i=4 j=1	i=5 j=1	i=6 j=1	i=7 j=1	i=8 j=1	i=9 j=1	i=10 j=1
j (Depth Direction)	i=1 j=2	i=2 j=2	i=3 j=2	i=4 j=2	i=5 j=2	i=6 j=2	i=7 j=2	i=8 j=2	i=9 j=2	i=10 j=2
	i=1 j=3	i=2 j=3	i=3 j=3	i=4 j=3	i=5 j=3	i=6 j=3	i=7 j=3	i=8 j=3	i=9 j=3	i=10 j=3
	i (Transverse Direction)									

Fig. 4: Illustration of the distribution of cohesive elements across rows (i) and columns (j) within the overlay.

4. Limit State Approach

Repetitive wheel loadings lead to reflective cracking. Because of the complexity of the fracture analysis simulation caused by this kind of loading, the permitted number of traffic passes (N_f) for a single wheel load event is determined using the limit state technique, as shown in Equation (2) [7, 9]. A single axle load with dual tires and an 80 KN weight was used to estimate the propagation of reflecting cracks. The limit state method assumes an unchanging contact area where the wheel load tire contact pressure is progressively increased until an RFA traffic value of 100 is reached, the material parameter, n, ranges from 2.35 to 4.27. These values are obtained from laboratory experiments. The Tseng and Lytton approach was used to calibrate the value of n in pavement modeling [7, 9, 18, 19].

$$N_f = (P_{80})^n \tag{2}$$

A higher N_f value means that the pavement can withstand more repeated loading cycles before failure occurs, indicating a longer service life and improved performance. This directly affects the overlay's ability to manage traffic-induced stresses over time. In practical terms, increasing N_f implies that the overlay can tolerate higher traffic loads without the formation of reflective cracks, thereby reducing the frequency of required maintenance interventions. By optimizing parameters such as overlay thickness and material modulus to achieve a higher N_f , engineers can effectively extend the lifespan of the pavement and minimize overall maintenance costs, contributing to better allocation of resources and less traffic disruption.

5. Modelling Asphalt Overlays Using Finite Elements

In this research, a three-dimensional model of finite elements was created using the Abaqus program, where a section of the road was represented with a length of five meters and a width of five meters for full-size scale, such that the asphalt covering layer (overlay) to be covered rests on top of a rigid pavement layer with joints. Also studying the properties of the RFA properties by making a half section to study the effect of the most important factors that contribute to the growth of reflective cracks by changing the thickness of the layers and comparing them to the RFA for each case. The

dimensions and properties of the model were selected to be compatible with the finite element model for each of Baek and Diallo [2, 7].

5.1 Model properties

A three-dimensional FE (Finite Element) model was constructed to simulate HMA (Hot Mix Asphalt) overlay on a JCP (Jointed Concrete Pavement) [7]. The pavement structure consists of four layers: a 30 to 100 mm thick HMA overlay, two concrete slabs each 200 mm thick, a base layer 200 mm thick, and a subgrade layer 3300 mm thick. The properties of the used material as shown in Table 1. Key features include a 10 mm wide full-cut construction joint placed transversely every 5.0 m to explore vulnerabilities related to reflective cracking. The model intentionally excludes dowel bars and aggregate interlocking to enhance the focus on joint stiffness. Additionally, the model incorporates the dimensions of a geometrically symmetric one-lane concrete slab measuring 5.0 m in length and 3.5 m in width for the full scale. While the half scale is 5.0 m in length and 1.75 m in width. The response of the overlay under the influence of changing properties of used materials and increasing the traffic load is proposed to be studied.

Table 1: Materials properties.

Layer	Elastic Modulus	Poisson's ratio	Thickness
Asphalt overlay	1500, 3000, 4500, 6000	0.35	30- 100 mm
Portland cement concrete	35000, 28000, 22000	0.2	200 mm
Granular base	300	0.4	200 mm
Subgrade	150	0.45	3300 mm

The vehicle load was simulated statically using dual tires with a tire pressure of 700 kPa and a wheel load of 40 KN, with the contact area shown in Figs. 5 and 6. This study applied uniform pressure to rectangular areas, approximating the dimensions of a single tire's contact area [20].

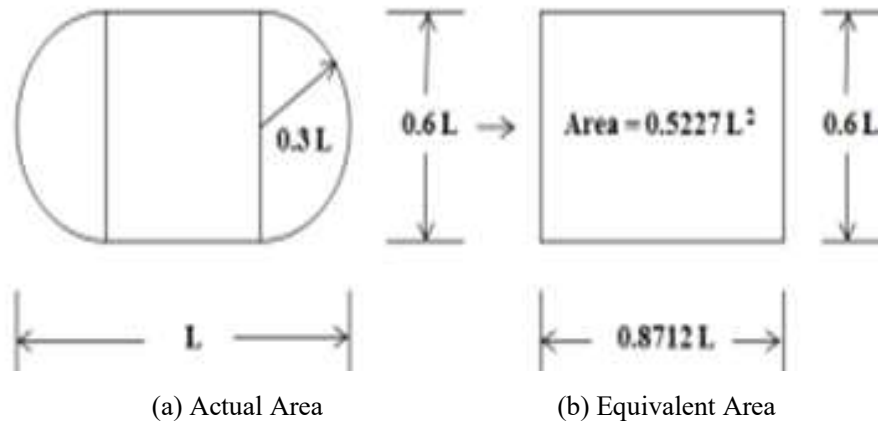


Fig. 5: Dimension of tire contact area between tire and pavement surface.

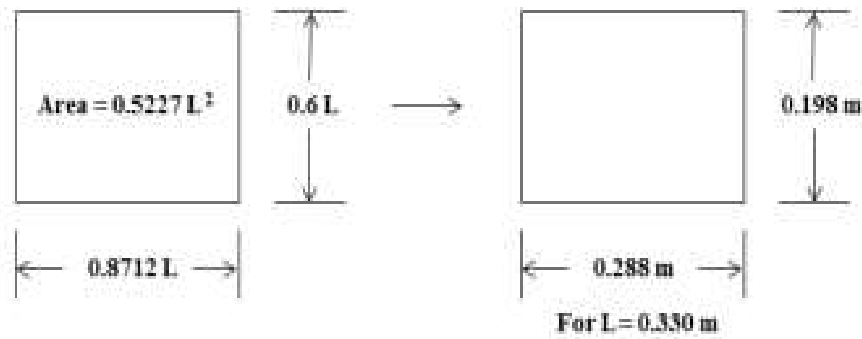


Fig. 6: Dimension of tire contact area used.

5.2 Boundary conditions and meshing techniques

In the full-scale pavement model, fixed boundary conditions, where all displacement components (u_x , u_y , u_z) and rotational components (θ_x , θ_y , θ_z) are set to zero, are applied to the bottom of the subgrade. Meanwhile, the edges of the HMA overlay, jointed concrete pavement and base layer are allowed to move without restriction, as shown in Fig. 7. In the case of the half-size pavement model, different conditions were enforced: along the x-z planes, a symmetric boundary condition along the x-axis ($u_y = 0$, $\theta_x = \theta_z = 0$) is applied, and along the y-z plane, a y-axis symmetric boundary condition ($u_x = 0$, $\theta_y = \theta_z = 0$) is implemented as shown in Fig. 8. Continuum elements in the model were defined using the eight-node brick element with reduced integration (C3D8R), which was utilized for modeling the asphalt and concrete layers. Additionally, a cohesive zone model was applied using the zero-thickness, eight-node three-dimensional cohesive element (COH3D) to simulate the path of reflective cracking. These elements were specifically placed in the asphalt overlay across the transverse joint, as shown in Fig. 9. Fine meshing was implemented along the wheel footprint and near potential cracks to ensure numerical convergence, as shown in Fig. 10.

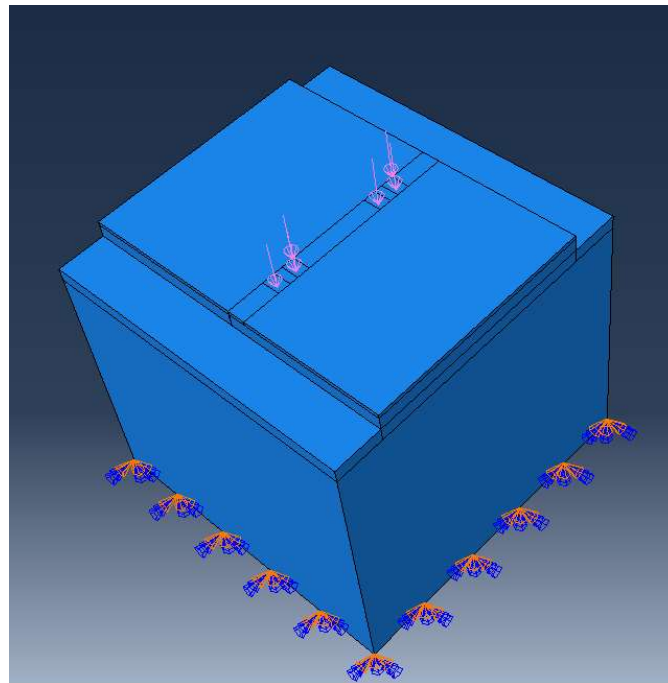


Fig. 7: Boundary Conditions for full-scale pavement model

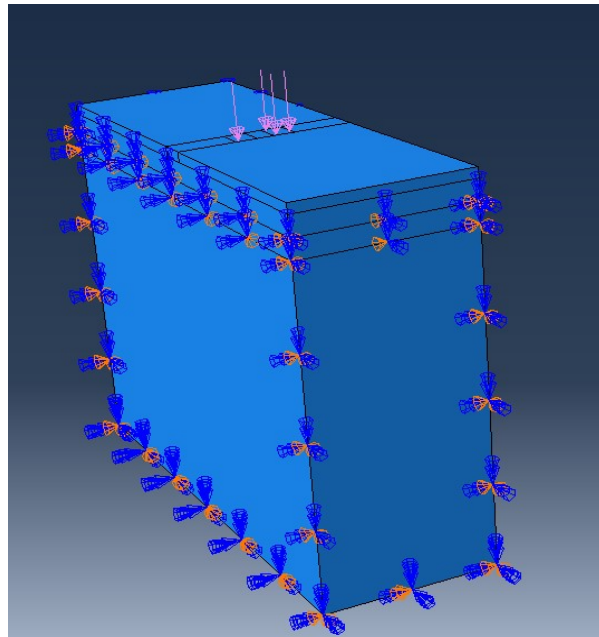


Fig. 8: Boundary Conditions for half-size pavement model.

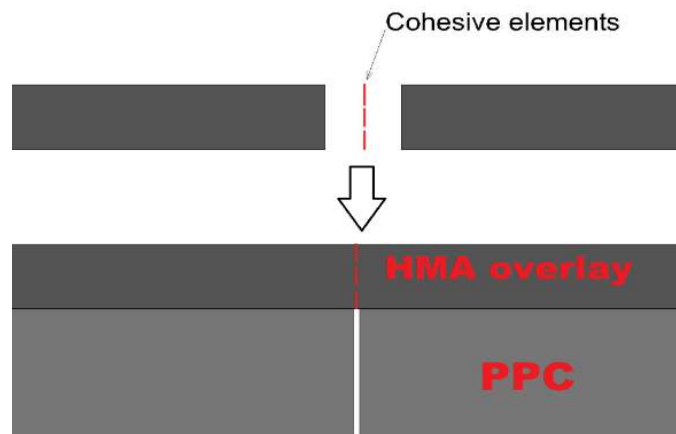


Fig. 9: Cohesive elements positioned at a possible reflective cracking location within the HMA overlay.

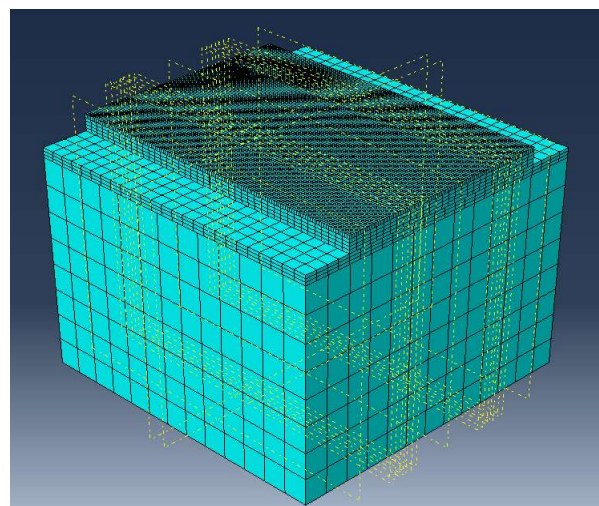


Fig. 10: Full-scale model meshes.

5.3 Interface model

One important factor to take into account for design and analysis is pavement layer interaction, the assumption that the pavement layers are fully bonded. Perfect adhesion between two layers is expected when layers, such as an asphalt overlay over existing concrete pavement, are thought to be fully bonded [2].

5.4 Model validation

In this study, we validated our three-dimensional finite element model (FEM) by comparing it with Baek's methodology and material properties, while introducing key differences in mesh density and geometry. To ensure a meaningful comparison, both models utilized the same material properties and a fracture energy of 270 J/m². The primary difference was that Baek's model used a viscoelastic material for the overlay layer, whereas our model employed a linear elastic material. Under a load of 80 kN, our model predicted a critical parameter value of 18.8, compared to 16.8 in Baek's results. Regarding the number of cycles to failure N_f , Baek's model predicted 144,062 cycles, while our model yielded a closely matching result of 144,656 cycles. To achieve this close agreement, we adjusted the n parameter in our fatigue model to 4.05, compared to Baek's value of 4.21 as shown in Table 2. The n parameter is a material constant that influences the fatigue life prediction. Despite the difference in material models (linear elastic versus viscoelastic), our FEM results closely matched those of Baek's model. This strong agreement demonstrates the robustness of our FEM approach [7].

6. Results and Discussion

Pavement responses of HMA overlay with 60 mm thickness by an 80-kN single-axle dual-tire loading in the full-scale and half-scale pavement models are compared. Surface deflections on the HMA overlay directly over the joint are plotted in Fig. 11 along the entire HMA overlay width of 3.5 m. where surface deflections are symmetric to the longitudinal centre line of the pavement in the full-scale pavement mode. This step is done first to verify the feasibility of using the half model by checking the displacement in both the half model and the full model. The displacement in the full model was approximately 0.3015 mm, while in the half model, it was about 0.303 mm, with a difference of around 0.5%.

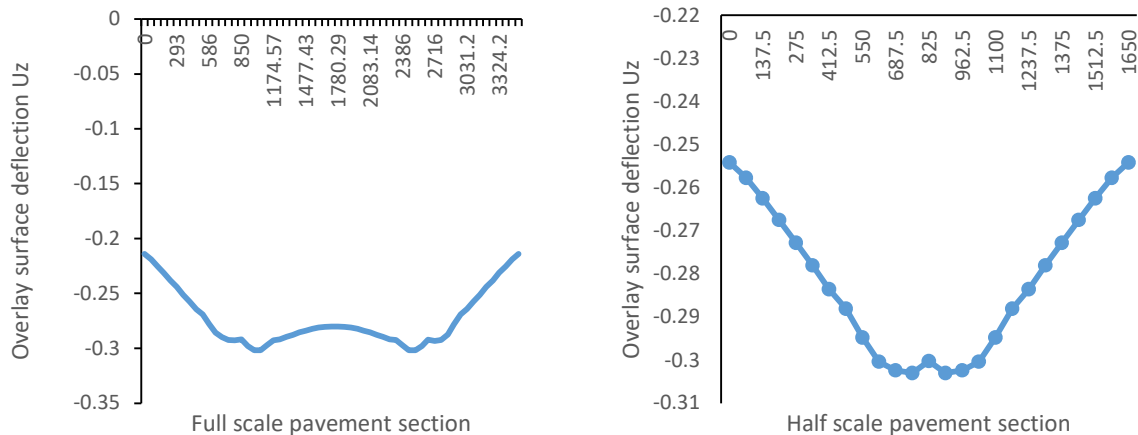


Fig. 11: Comparison of the full-scale and half-scale pavement model for surface deflection.

6.1 Critical axle load position and critical response

To identify the critical position of the wheel load, four scenarios with S distance were considered: the first position directly at the concrete joint (S=0 mm), the second at a distance of S=144 mm, the third at S=432 mm, and the fourth at S=720 mm, where S is the distance measured from the geometric centre of the wheel to the centre of the joint. The results showed that when the axle load was applied to one side of the joint position 2, it had the greatest effect. With measurements of 88 $\mu\epsilon$ (microstrain) for longitudinal strain. At position 1, the longitudinal tensile strain was 78 $\mu\epsilon$, and the measured longitudinal tensile strain was nearly 60 $\mu\epsilon$ and 30 $\mu\epsilon$ for the other two positions, as shown in Fig. 12.

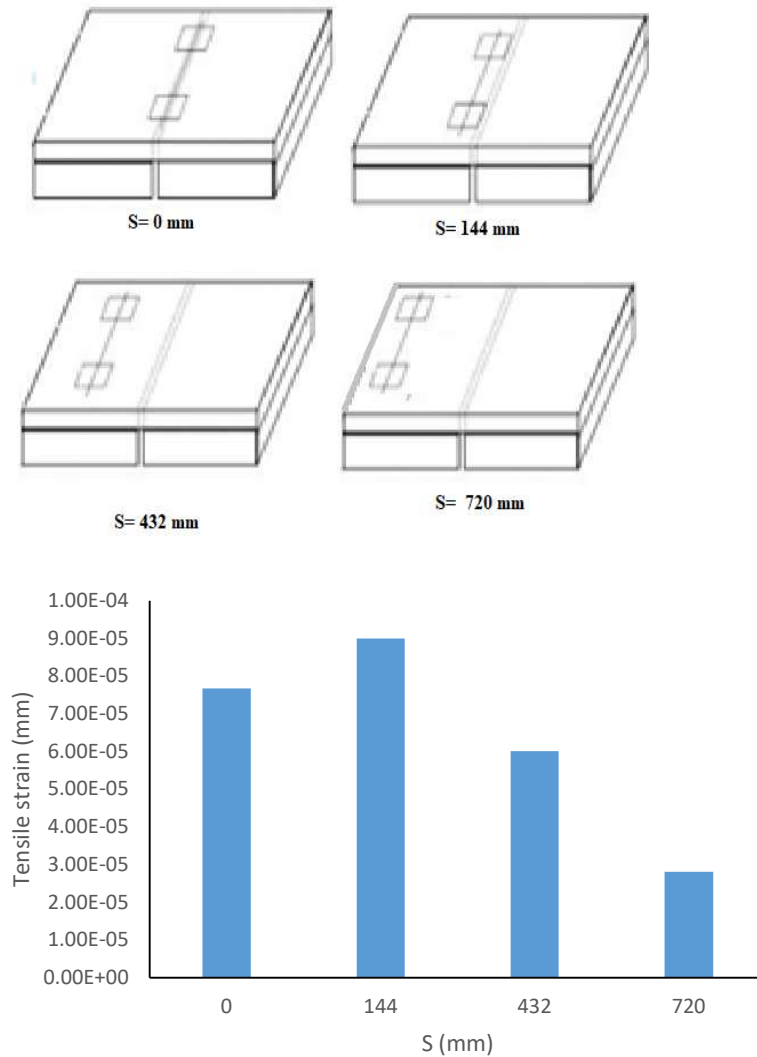


Fig. 12: Critical Axle Load Position and Corresponding Longitudinal Strain Response at Transverse Joint.

6.2 Effect of the asphalt overlay thickness and its elastic modulus

Fig. 13 illustrates the variation of tensile strain at the bottom of the overlay with varying asphalt overlay thicknesses and asphalt modulus. For asphalt overlay elastic moduli of 1500 MPa, 3000 MPa, 4500 MPa, and 6000 MPa with corresponding thicknesses of 30 mm, 60 mm, and 100 mm, the tensile strain magnitude ranges from 36.5 $\mu\epsilon$ to 416.5 $\mu\epsilon$. This significant variation in pavement response due to changes in overlay thickness and modulus underscores the critical role of asphalt overlay design in pavement performance. Specifically, as the asphalt overlay thickness increases, the tensile strain magnitude decreases, independent of the asphalt overlay material's modulus. Conversely,

increasing the asphalt material modulus also results in decreased tensile strain. For instance, with an asphalt overlay thickness of 30 mm, increasing the asphalt overlay modulus from 1500 MPa to 6000 MPa reduces the tensile strain by approximately 37.5%. Moreover, for an asphalt overlay modulus of 4500 MPa, increasing the asphalt overlay thickness from 30 mm to 100 mm leads to a reduction in tensile strain magnitude by about 68.8%. It's also noteworthy that tensile strain reduction due to changes in asphalt overlay modulus becomes more pronounced as the overlay thickness exceeds 100 mm. For example, with a 60 mm asphalt overlay thickness, changing the asphalt overlay modulus from 1500 MPa to 6000 MPa results in a strain reduction of 70%.

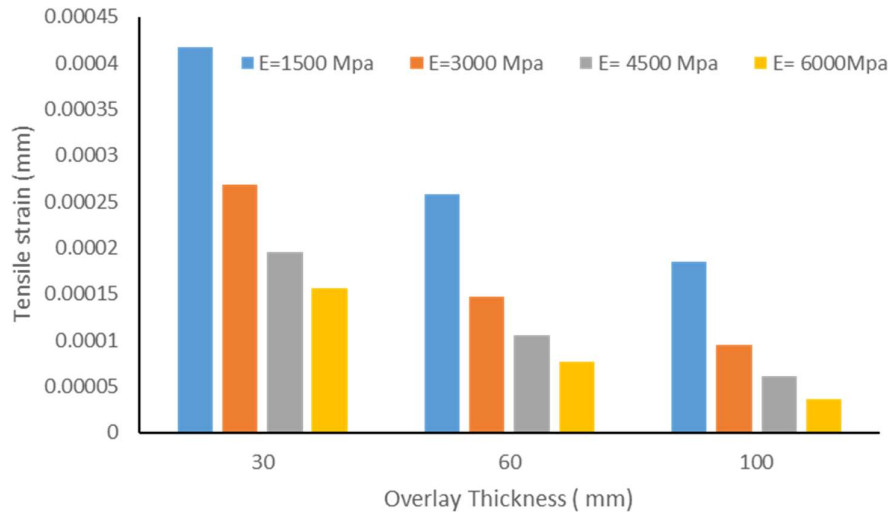


Fig. 13: shows the variation of produced strains due to thickness and elastic modulus variation.

6.3 Effect of the existing JPC modulus

The effect of the rigidity of the existing joint pavement concrete (JPC) layer was evaluated by considering three different JPC moduli: 22,000 MPa, 28,000 MPa, and 35,000 MPa. The analysis results, as shown in Fig. 14, indicate that higher PCC elastic moduli yield better performance compared to lower moduli. This is demonstrated with an overlay set at a thickness of 60 mm and a modulus of $E = 6000$ MPa, emphasizing how variations in the PCC material properties significantly influence strain distribution.

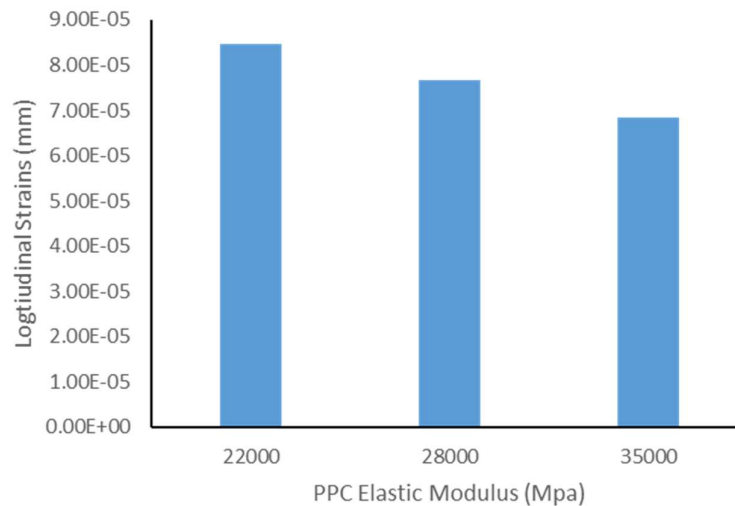


Fig. 14: Compares the relationship between the phase of PPC materials and the strains produced at the bottom of the AC overlay.

6.4 Effect of the joint width

The width of the joint or crack is another factor representing the condition of the existing PCC pavement. Fig. 15 shows the AC tensile strain at the bottom of the overlay versus the joint width for different overlay thicknesses. When increasing the joint width from 6 mm to 20 mm, the magnitude of the tensile strain increased at the same overlay thickness.

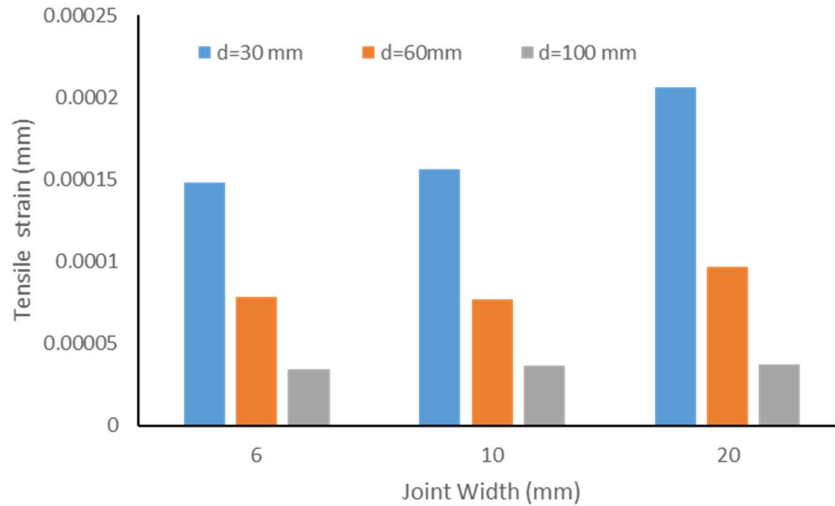


Fig. 15: Compares the relationship between the Joint width and the strains produced at the bottom of the AC overlay. For Ac modulus $E = 6000$ MPa.

6.5 Representative fracture area (RFA)

The RFA was computed at the end of the loading phase, with particular attention to how it changed about a normalized axle load of 80 KN (P80) where fracture energy was 590 j/m and elastic modulus 6000 MPa. Table 2 illustrates the impact of increasing the multiplier by a factor of axel load 80 kN, from one time up to 25 times, on the RFA. When the fracture area reaches 99%, the crack becomes entirely brittle. The analysis was conducted across various asphalt thicknesses, including 30 mm, 60 mm, and 100 mm. Results indicate that the RFA is strongly influenced by asphalt thickness, confirming the hypothesis that greater asphalt thickness reduces the likelihood of reflective crack.

Table 2: values of RFA %

Thickness (mm)	RFA%	P80	n	N_f	G_f N/mm2	Notes
60	99	16.8	4.21	144,062	270	Back2010 [7]
60	99	18.8	4.05	144,656	270	
30	99	10	4.05	1.12×10^4	590	
60	99	20	4.05	2.26×10^5	590	
100	99	25	4.05	4.59×10^5	590	

6.6 Determination of the number of load repetitions to failure

To calculate the load repetition value, we used Equation (2). The average value of the n parameter was assumed to be 4.05, and the P80 value was calculated from Table 2. Fig. 16 shows the number of load repetitions that cause reflective cracking at different asphalt thicknesses. It is clear that as the thickness increases, more load repetitions are needed to cause reflective cracking. For example, at 30 mm thickness, the load repetition value is 1.12×10^4 , at 60 mm thickness, it is 2.26×10^5 , and at 100 mm thickness, it is 4.59×10^5 .

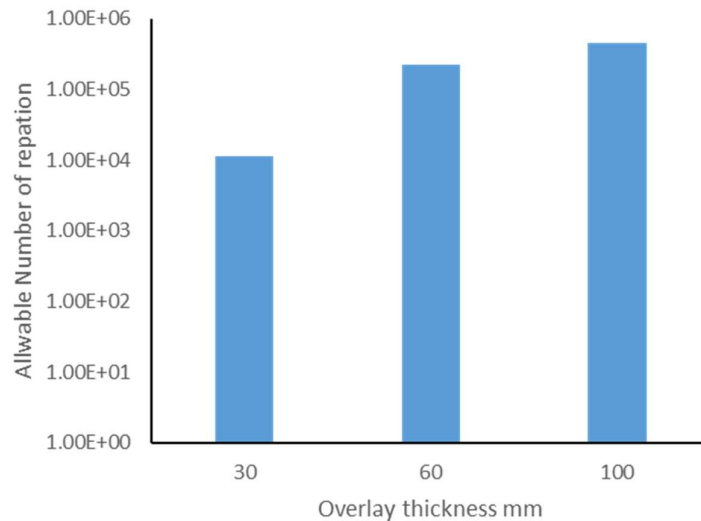


Fig. 16: Estimation of N_f with different AC overlay thickness.

7. Conclusion

Using the Finite Element model, this study improved understanding of the fracture mechanism in the Hot Mix Asphalt (HMA) overlay on jointed plain concrete (JPC), with a consideration of the development of reflective cracks. This study investigated the way reflective cracking progresses in different cases and the effects of various factors such as traffic load, overlay thickness and its modulus of elastic, foundation elastic modulus, joint width, and load positions. The key findings of this study are as follows:

- When the axle load was applied to one side of the joint it had the greatest effect.
- Regardless of the modulus of the asphalt material when increasing the thickness of the overlay the magnitude of the tensile strain decreases.
- When the asphalt material modulus increases the tensile strain decreases depending in asphalt thickness.
- Existing JCP's bearing capacity has a significant impact on reflective cracking.
- The highest values of JPC elastic modules are better than the lowest which gives low strain values.
- It was clear that the CZM governed by a bilinear traction separation law (TSL) was able to predict the fracture behavior of HMA.
- One pass of 80-kN-axle loading did not damage the HMA overlay. The resulting traction force in cohesive elements was lower than the HMA strength.
- Results indicate that the RFA is strongly influenced by asphalt thickness, confirming the hypothesis that greater asphalt thickness reduces the likelihood of reflective crack.
- It is clear that as the thickness increases, more load repetitions are needed to cause reflective cracking.

References

- [1] Y. S. Ajool, A. A. Allawi, and A. H. Kalil, "Mitigation of Reflection Cracking in Asphalt Concrete Overlay on Rigid Pavements," in *E3S Web of Conferences*, 2023, vol. 427: EDP Sciences, p. 03004 .

- [2] A. O. Diallo and M. V. Akpınar, "Mechanistic Responses of Asphalt Concrete Overlay Over Jointed Plain Concrete Pavement Using Finite Element Method," *The Baltic Journal of Road and Bridge Engineering*, vol. 15, no. 5, pp. 80-93, 2020.
- [3] Z. Ghauch and G. Abou-Jaoude, "Strain response of hot-mix asphalt overlays in jointed plain concrete pavements due to reflective cracking," *Computers & Structures*, vol. 124, pp. 38-46, 2013.
- [4] F.-L. Tsai, R. L. Lytton, and S. Lee, "Prediction of reflection cracking in hot-mix asphalt overlays," *Transportation Research Record*, vol. 2155, no. 1, pp. 43-54, 2010.
- [5] J.M. A. S. Hadi and M. H. Al-Sherrawi, "The Influence of Base Layer Thickness in Flexible Pavements," *Engineering, Technology & Applied Science Research*, vol. 11, no. 6, pp. 7904-7909, 2021.
- [6] A. H. Albayati, Y. S. Ajool, and A. A. Allawi, "Comparative Analysis of Reinforced Asphalt Concrete Overlays: Effects of Thickness and Temperature," *Materials*, vol. 16, no. 17, p. 5990, 2023.
- [7] J. Baek, *Modeling reflective cracking development in hot-mix asphalt overlays and quantification of control techniques*. University of Illinois at Urbana-Champaign, 2010.
- [8] M. R. Taha, S. Hardwiyono, N. I. M. Yusoff, M. R. Hainin, J. Wu, and K. A. M. Nayan, "Study of the effect of temperature changes on the elastic modulus of flexible pavement layers," *Research Journal of Applied Sciences, Engineering and Technology*, vol. 5, no. 5, pp. 1661-1667, 2013.
- [9] J. Baek and I. L. Al-Qadi, "Mechanism of overlay reinforcement to retard reflective cracking under moving vehicular loading", *Pavement Cracking Mechanisms, Modeling, Detection, Testing and Case Histories*, pp. 563-573, 2008.
- [10] L. Guo, J. Yue, P. Guo, and X. Wang, "Multiple Reflective Cracks in Semirigid Base Asphalt Pavement under Traffic Load Using XFEM," *Advances in Civil Engineering*, vol. 2022, 2022.
- [11] M. Rith and S. W. Lee, "Development of cohesive-zone-based prediction model for reflective cracking in asphalt overlay," *International Journal of Pavement Engineering*, vol. 23, no. 4, pp. 1050-1059, 2022.
- [12] A. International. "ASTM D7313-13: Standard test method for determining fracture energy of asphalt-aggregate mixtures using the disk-shaped compact tension geometry." <https://www.astm.org/d7313-13.html> (accessed.
- [13] S. H. Song, G. H. Paulino, and W. G. Buttler "A bilinear cohesive zone model tailored for fracture of asphalt concrete considering viscoelastic bulk material," *Engineering Fracture Mechanics*, vol. 73, no. 18, pp. 2829-2848, 2006.
- [14] C. Du, Y. Sun, J. Chen, H. Gong, X. Wei, and Z. Zhang, "Analysis of cohesive and adhesive damage initiations of asphalt pavement using a microstructure-based finite element model," *Construction and Building Materials*, vol. 261, p. 119973, 2020.
- [15] N. Han, L. Fan, and Y. Zhang, "Estimation of cohesive zone model parameters for glass/Elium composites with different processing temperature," *Journal of Reinforced Plastics and Composites*, vol. 43, no. 11-12, pp. 601-611, 2024.
- [16] M. A. Elseifi, J. Baek, and N. Dhakal, "Review of modelling crack initiation and propagation in flexible pavements using the finite element method," *International Journal of Pavement Engineering*, vol. 19, no. 3, pp. 251-263, 2018.
- [17] B. Ding, X. Zou, Z. Peng, and X. Liu, "Evaluation of Fracture Resistance of Asphalt Mixtures Using the Single-Edge Notched Beams," *Advances in Materials Science and Engineering*, vol. 2018, no. 1, p. 8026798, 2018.
- [18] R. L. Lytton, F. L. Tsai, S. I. Lee, R. Luo, S. Hu, and F. Zhou, "Models for predicting reflection cracking of hot-mix asphalt overlays," *NCHRP report*, vol. 669, pp. 48-56, 2010.
- [19] K.-H. Tseng and R. L. Lytton, "Fatigue damage properties of asphaltic concrete pavements," *Transportation Research Record*, no. 1286, 1990.
- [20] A. Nega and H. Nikraz, "Evaluation of tire-pavement contact stress distribution of pavement response and some effects on the flexible pavements," *Airfield and Highway Pavements 2017: Pavement Innovation and Sustainability*, pp. 174-185, 2017.

تقييم خصائص التغطية الأسفلتية على سلوك التشققات الانعكاسية في الرصف المركب باستخدام نمذجة العناصر المحدودة

ملخص

إن طريقة التغطية الأسفلتية واحدة من أكثر الطرق شيوعاً في إعادة تأهيل الأرصفة الصلبة، حيث تُعتبر طبقة التغطية الإسفلتية تقنية معيارية لاستعادة كفاءة الطريق وتحسين جودة القيادة. وعلى الرغم من فعاليتها المعروفة، تواجه هذه الطريقة تحدياً يتمثل في المشكلة المستمرة المتمثلة في التشقق الانعكاسي.

باستخدام تحليل العناصر المحدودة (FEA) مع نموذج المنطقة المتماصة (CZM). تم تطوير نموذج شامل ثلاثي الأبعاد باستخدام برنامج الأباكوس لمحاكاة مقطع طريق بطول خمسة أمتار، متضمناً سماكات مختلفة لطبقة الاضافيه الأسفلتية (٣٠ مم، ٦٠ مم، و ١٠٠ مم) ومعامل مرنة (١٥٠٠ ميغا باسكال إلى ٦٠٠٠ ميغا باسكال) موضوعة فوق ارصفه خرسانية متدهوره. تمت صياغة أحمال المركبات باستخدام إطارات مزدوجة مع ظروف ضغط وحمل محددة. كشفت النتائج أن زيادة سماكة الطبقة الاضافيه الاسفلتية يقلل بشكل كبير من إنفعالات الشد المتولده في طبقة الاضافه الاسفلتية واحتمالية التشقق الانعكاسي، خاصة عندما يتم تطبيق أحمال المحور بالقرب من المفاصل. وكذلك دور زياده معامل المرنة في طبقة الرصف الخرساني القديمه و تقليل عروض الفواصل الخرسانيه على تعزيز أداء الرصف. أظهر إدخال مقياس منطقة الكسر التمثيلي (RFA) أن زيادة سماكة الأسفلت تقلل بشكل كبير من تطور انتشار الشقوق غير المنتظم، وبالتالي زيادة عدد مرات تكرارات الحمل حتى الفشل ما يعني تعزيز متانة الرصف. في النهاية، خلصت الدراسة إلى أن تحسين كل من سمك وخصائص المواد لطبقة التغطية الأسفلتية أمر بالغ الأهمية لتخفيف التشققات العاكسة، وإطالة عمر الرصيف، مما يساهم في تقليل تكاليف الصيانة، وبالتالي توفير إرشادات قيمة لتصميم رصف أكثر متانة وفعالية من حيث التكلفة.